Data-Driven Studies of Noisy Chaotic Oscillators

Daniel Xu[1], Luca Nijim[2], Abjini Chattopadhyay[3], Maria Cameron[4]

[1]Columbia University, [2]University of Notre Dame, [3]Montgomery Blair High School, [4]University of Maryland

Introduction

Chaotic behavior is observed in a diverse range of mechanical and non-mechanical systems, such as thermal pulse combustors and living organisms. Understanding these complex dynamical systems pose challenges due to sensitivity to initial conditions. This study focuses on analyzing non-autonomous systems, particularly harmonically forced Duffing oscillators as representative examples.

The mathematical form of the noisy Duffing oscillator is described by the equation

$$\ddot{x} + c\dot{x} + k_1 x + k_3 x^3 = \gamma\cos(\omega t) + \sigma\eta_t,$$

where c is the viscous damping, k_1 is the linear stiffness parameter, k_2 is the nonlinear stiffness, γ is the forcing amplitude, ω is the forcing frequency, σ is the noise level, and η_t is the standard Brownian motion.

To understand the complex behavior and transitions between different states in noisy Duffing oscillators, we use Transition Path Theory (TPT), which offers a framework to study transitions between two subsets of interest, often labeled as sets A and B. A central concept of TPT is the committor function, which characterizes the probability of the system ending up in set A or B given a starting point outside of $A \cup B$. This approach provides insights into the dynamics and probabilities of state transitions.

In the original context, obtaining the committor function as the solution of a boundary value problem of an elliptic partial differential equation (PDE) poses significant challenges and is impractical for many real-world applications. To adddress this limitation, TPT can be adapted for discrete-time Markov chains, which is the approach used in this analysis. From the transition matrix P of the Markov chain, we construct the generator $L = P - I$ of the stochastic process. This allows us to compute the forward committor, which represents the probability of the process reaching set B before A when starting at state i. This is achieved by solving the following system of equations:

$$\sum_{k\in S} L_{ik} q_k^+ = 0, \forall i \in (A \cup B)^C \qquad q_i^+ = 0, \forall i \in A \qquad q_i^+ = 1, \forall i \in B.$$

Moreover, we extend our analysis to compute the backward committor and probability density of reactive trajectories through analogous techniques. In this manner, we strive to leverage the integration of Markov chains and TPT to develop a deeper understanding of the dynamics of state transitions in noisy Duffing oscillators. Given the prevalence of noisy chaotic oscillators in both natural and engineered systems, our research holds potential to provide insights for the design and control of such systems.

Simple Case: Only Periodic Invariant Sets

In this section, we explore simple invariant sets to establish a foundation for analyzing more complex behaviors. The system considered is described by the equation

$$\ddot{x} + 0.1\dot{x} + x + 0.3x^3 = 0.4\cos(1.4t) + \sigma\eta_t$$

Using a $\sqrt{0.05}$ noise level for analysis, we observe stable low and high amplitude periodic attractors, basin boundaries indicating regions of attraction, and a saddle point serving as a boundary between the periodic attractors.

Using a noise level of $\sqrt{0.01}$, we construct a point cloud using enhanced sampling to capture transitions and points around the attractors. Additionally, we calculate covariance ellipses to understand the attractor structure, as depicted in the plot below.

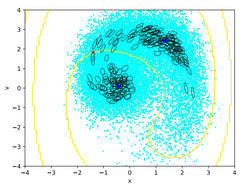

Figure 1. Point Cloud with Attractors and Basin Boundaries

Case Study I: Monostable Oscillator

In the non-noisy case with $k_1 > 0$ and $k_3 > 0$, the system behaves as a monostable Duffing oscillator with hardening characteristics. We follow the parameters from Agarwal's paper[2]:

$$\ddot{x} + 0.02\dot{x} + x + 5x^3 = \gamma\cos(0.5t).$$

Using γ as a control parameter, we varied its range to observe the system's chaotic response. The bifurcation diagram below reveals additional limit cycles (in green and orange) discovered using Newton's method, which were absent in Agarwal's paper. Focusing on $\gamma = 3.6$, we explored the coexistence of two attractors with fractal-like basin boundaries for deeper insights.

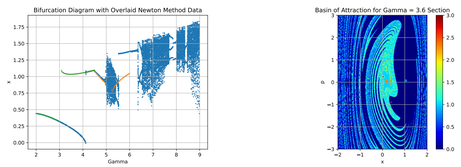

Figure 2. (a) Bifurcation Diagram and (b) Basins of Attraction

To study state transitions, we introduce a noise term of $\sqrt{0.04}\eta_t$ and construct a point cloud capturing transitions and points around the attractors.Using metadynamics and delta-netting techniques, we achieve a quasi-uniform point distribution. Subsequently, we compute the transition probability matrix by launching numerous trajectories from each point in the point cloud and monitoring their ending positions. The transition probability for a specific point i to j in the point cloud is determined based on the Mahalanobis distance of j to point i's trajectories' ending positions. Exponential weighting ensures probabilities decrease with distance, reflecting likelihood of transitions.

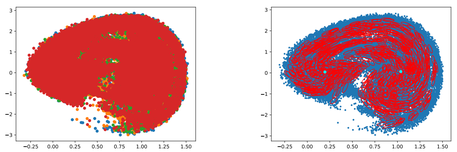

Figure 3. (a) Enhanced Sampling and (b) Stochastic Matrix

Using Tarjan's algorithm, we extract the largest strongly connected component within the point cloud, indicating a cohesive group with reciprocal transitions between its points. With the transition matrix, we calculate the forward and backward committor functions, delineating attractor A in magenta and attractor B in cyan. This analysis reveals the probabilities of reaching each attractor from any point in the system.

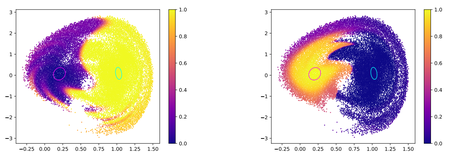

Figure 4. (a) Forward Committor and (b) Backward Committor

Continuing, we analyze the probability of each state being involved in a reactive trajectory. To gain insight into transition pathways, we simulate escape paths from attractor A to attractor B using the computed transition probabilities. This also serves as validation for our results.

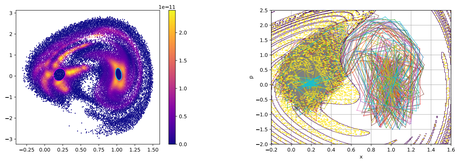

Figure 5. (a) Probability Density of Reactive Trajectories and (b) Escape Paths from A to B

Case Study II: Bistable Oscillator

Here $k_1 < 0$ and $k_3 > 0$, and the system behaves as a bistable Duffing oscillator with softening characteristics. The system is defined by the equation

$$\ddot{x} + 0.085\dot{x} - 0.5x + 0.2x^3 = \gamma\cos(0.42t)$$

The parameter γ is varied, creating interesting dynamics. We select the value $\gamma = 0.15$ because it generates three attractors: a positive and negative low-amplitude attractor as well as a high-amplitude attractor with intricate basin boundaries (Figure 6).

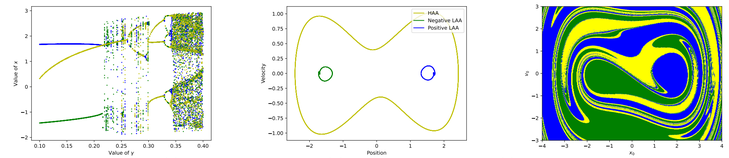

Figure 6. (a) Bifurcation Diagram, (b) Attracting Cycles, and (c) Basins of Attraction

To study transitions, a noise coefficient of $\sigma = 0.005$ is introduced, and increased to $\sigma = 0.05$ for sampling. After a quasi-uniform point distribution is achieved, we attempted to compute the means and covariances of one-period trajectories launched from each point, but noticed extreme variance in the eigenvalues of the covariance matrices. We observed that certain 'joker points', especially near to the basin boundaries, violated the assumption used in Case Study I that the one-period trajectories conformed to a Gaussian distribution.

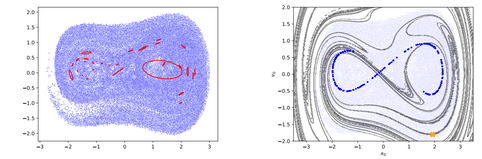

Figure 7. (a) Discrepancies in Covariance, and (b) 'Joker Points'

Because the exponential weighting method proved inviable, I used a nearest-neighbor method to compute the stochastic matrix: if n stochastic trajectories were launched from point i, and k of the trajectories landed nearest to point j, then $P_{ij} = \frac{k}{n}$. Using this stochastic matrix, I computed the committor function outlined earlier. Notably, the committor function proved to be almost exactly 0.5 across most of the state space, with few regions closer to 0 or 1. Notably, the points for which the committor function is closer to 0.5 are more likely to produce one-period trajectories with much greater covariance.

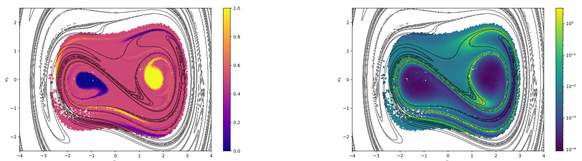

Figure 8. (a) Forward Committor Function, and (b) Magnitude of Greatest Covariance Eigenvalue

References

[1] B. Balachandran L. Cilenti, Maria Cameron.
Most probable escape paths in periodically driven nonlinear oscillators.
Chaos, 32(1):083140, 2022.

[2] B. Balachandran V. Agarwal, R. Wang.
Data driven forecasting of aperiodic motions of non-autonomous systems.
Chaos, 31(2):021105, 2021.

Acknowledgement: This work was supported by NSF REU grant DMS-2149913.

[1]xu.daniel@columbia.edu, [2]lnijim@nd.edu, [3]abjini.c@gmail.com [4]mariakc@umd.edu